International Journal of Numerical Methods and Applications
Volume 3, Number 2, 2010, Pages 151-172
Published Online: August 29, 2010
This paper is available online at http://pphmj.com/journals/ijnma.htm

A BEM-BASED INVERSE METHOD FOR DISCONTINUITY DETECTION IN ACOUSTIC MEDIA

TOAN DUC CAO and TINH QUOC BUI*

Faculdade de Engenharia
Universidade Católica Portuguesa
Palma de Cima
1649-023 Lisboa, Portugal

Chair of Structural Mechanics
Department of Civil Engineering
University of Siegen
Paul-Bonatz Str. 9-11
D-57076, Siegen, Germany
e-mail: tinh.buiquoc@gmail.com

Abstract

The paper presents an inverse procedure for the detection of discontinuity geometries by means of the boundary element method in acoustic media. The problem is aimed at determining of the existence of a hidden hole or a flaw within an elastic plate structure. Within this technique, the outer boundary of considered problems is fixed at initial known nodes, while the remaining unknown nodes on the boundary are computed during the implementing process and other internal nodes of the domain are determined by the interpolation of the boundary element method. The core of the technique is that basing upon the estimation of the loss of acoustic pressure at surrounding regions of flaw or hole. In the current situation of the method, two individual models based on the boundary element method

2010 Mathematics Subject Classification: 74S30, 74K20.

Keywords and phrases: boundary element method, acoustic media, inverse analysis, flaw detection.

*Corresponding author

Received April 3, 2010

with and without flaw or hole must be solved simultaneously. The shape and location of flaw and hole, area and radius of the hole as well as the length and the angle for the flaw can be identified. Several numerical examples are given to demonstrate the applicability and the effectiveness of the proposed method.

1. Introduction

Many physical phenomena encountered in sciences and engineering can be described in terms of partial differential equations (PDEs). Over the last decades, many numerical methods have been found and developed to solve a wide class of different physical problems through those PDEs. They are useful and always be improved and studied ceaselessly. The boundary element method (BEM) [1, 2] is one of the most effective methods and becomes an important technique in solving of such physical problems. Unlike the traditional finite element methods (FEM) [3], extended finite element method (X-FEM) [4, 5], or meshfree methods [6, 7] a mesh of the boundary of relevant domains is required for the BEM method. Another advantage compared to those of other approaches can easily be seen that the discretization of the BEM only occurs on the surfaces rather than over the entire domain.

In terms of the BEM, the PDEs are, in general, formulated as integral equations, i.e., in boundary integral forms. The integral equation may be regarded as an exact solution of the governing PDEs. In order to fit boundary values into the integral equation, the BEM is attempted to use the given boundary conditions. Nevertheless, the BEM can be applied in various areas of engineering problems including heat transfer, fluid mechanics [1], contact problems, fracture mechanics [8], electromagnetic field, piezoelectric materials [9, 10], stress analysis [11] and acoustics [12, 13], which is the major subject of the present study. Further applications can be found, see, e.g., in [1, 9, 13] as well as its disadvantages and advantages compared to those of FEM can also be found in [14].

As said above, the acoustic media is the main task and treated in this work, which is an important branch within the sphere of physical problems. An acoustic field can exist within a fluid or a solid domain, where wave equation can often be formed as acceptable models with respect to problems of acoustic media. The wave equation of that acoustic field is usually reduced to a sequence of Helmholtz equations system. With the current capability of the BEM, such Helmholtz equations

derived from the discretization of considered structural acoustic problems can be solved approximately [14]. With respect to the BEM-based applications in acoustic media, a brief discussion of its developed history can be found in [12]. Furthermore, Cheng and Cheng [15] recently presented a deep of heritage and early history of the BEM.

In the perspective of inverse problems for flaw detection in solid structures using the BEM, Nishimura and Kobayashi [16] proposed a boundary integral equation method where the shape and the location of flaws were determined by minimizing the error of a certain boundary integral equation. The geometry of the flaw was additionally determined from the experimental data. In the same manner Bezerra and Saigal [17], who presented an inverse procedure in terms of such optimization problems with the objective function being the sum of the squares of the differences between the measured and the computed displacements for an assumed flaw configuration. With this procedure, the geometric condition that the flaw lying within the domain of the object was imposed using an internal penalty function. Mellings and Aliabadi [18] also introduced a new boundary element formulation, a dual BEM. This method was used to identify the location and size of internal flaw in two-dimensional structures, in which an inverse analysis based on optimization method, was proposed. Other interested studies using genetic optimization or artificial neural network for identifying of flaw by means of BEM can also be found in [19, 20].

As known that discontinuity detection problems always play a significant role in reality. They help to detect flaws within a structure, which are usually the derivation of the failure of such structure. In principle, the problems of discontinuity detection or flaw identification can be a specified case and belong to the class of the inverse problems. In this task, a given model of a certain system is defined and its outputs are available, but the value of the parameters involved in the assigned system are unknown, which must be determined [18, 20]. In our studies, on the one hand, the BEM is employed in solving forward problems to obtain the relevant parameters such as the energies of sound-pressure; on the other hand, the other relevant unknown parameters on the boundary of the problems are determined by the inverse method. This inverse method can be found in [21, 22] studying on experimental flaw identification using electrical impedance tomography. We now first introduce such inverse technique in acoustic media using the BEM in the present work. The details of the method are given deeply in Section 3 of the paper.

In other words, discontinuity detection is required on structural components and for which a variety of methods is available. Usually, non-destruction testing methods are often employed to deal with for such detection of hidden flaws without any damage of the structures. Some of the common non-destruction testing methods are based on the techniques of visualization of flaws such as dye penetrates, magnetic particles, eddy current, ultrasonic and radiographic. Due to their capability, they can, in some cases, give accurate information about the approximate position of the flaw, but in other cases, the information they provide is usually limited [18, 21, 22]. Alternatively, as mentioned above, the goal of the present work is attempted to propose an inverse method to discontinuity detection through the BEM. This approach is able to detect the discontinuities of the existence of a hidden hole or a flaw within specified elastic structures, in which the shape and the location as well as the length and the angle for flaw problem can be identified. It may provide an effective tool for the non-destruction testing and monitoring of the structures.

The outline of this paper followed the introduction that goes as follows: In Section 2, a brief description of the BEM involving the formulation of Helmholtz's equation describing the structural acoustic is given. In Section 3, an inverse method including its algorithm describing the method is presented. Numerical examples are given in the next section. We shall end by a conclusion and discussion involving future works.

2. Boundary Element Formulation for Helmholtz's Equation

In this section, the BEM formulation for Helmholtz equation is briefly given. More details can be found in standard textbooks, see, e.g., [1, 2, 10, 24, 25]. In general, the BEM consists of two main approaches differently. One is the so-called direct approach, sometimes known as interior problems, which is considered in our study and the other is the indirect one or exterior problems [2, 14]. The underlying problem addressed in this section is that of computing an acoustic pressure field within a homogeneous isotropic solid domain subjected to a specified boundary condition. The domain of the interior acoustic problem occupies an arbitrary closed domain V with its closed boundary $S = S_p \bigcup S_v$. The acoustic pressure field is often taken to be formed by a corresponding wave equation. In most typical applications, acoustic problems are well modeled by the Helmholtz's equation [1, 2, 24]

$$(\nabla^2 + k^2)\, p = 0 \ \text{ with } \ p \in V \tag{1}$$

here p is the acoustic pressure subjected on S_p and k stands for the wave number expressed by $k = \omega/c,$ in which ω and c are the angular frequency and the speed of sound in acoustic medium, respectively [12, 23]. In this study, the bounding surface is subjected by an acoustic pressure field on S_p and a normal velocity v on S_v with $\hat{i}$ is the complex number and ρ is the density of solid medium [12],

$$v = \frac{\hat{i}}{\rho\omega}\frac{\partial p}{\partial n} \quad \text{on} \quad S_v. \tag{2}$$

The basic idea of the BEM is that the PDEs governing the solution in a domain (1) can be replaced by an equation that governs the solution on the boundary alone. Accordingly, a free-space Green's function g in terms of the Dirac delta function $\delta(R - R_0)$ is introduced. Here R_0 and R are the initial and current radiate radius of acoustics, respectively,

$$(\nabla^2 + k^2)\, g(|\, R - R_0\,|) = -\delta(R - R_0). \tag{3}$$

By making use of the solution of the Green's function, the Helmholtz integral equation (1) for acoustic problems becomes

$$cp(R) = \int_S \left(p(R_0)\frac{\partial g}{\partial n} - g(|\, R - R_0\,|)\frac{\partial p}{\partial n}\right) dS \tag{4}$$

here n is unit normal vector on boundary S, and coefficient c depending on the current position of the radiate radius R, is given [1]

$$c = \begin{cases} 1, & \text{for } R \text{ inside } V, \\ 1/2, & \text{for } R \text{ on the boundary } S, \\ 0, & \text{for } R \text{ outside } V. \end{cases} \tag{5}$$

The BEM formulation is then transformed from a system of continuous equation into a corresponding discrete system. The purpose is to find an equation system in which the unknown boundary node values are determined. The boundary is now discretized by M boundary elements with a total of N boundary nodes, the Helmholtz discrete integral equation can be obtained [2]

$$cp_i - \sum_{j=1}^{N} \int_{S_j} p_j \frac{\partial g}{\partial n}\, dS = -\sum_{j=1}^{N} \int_{S_j} g \frac{\partial p}{\partial n}\, dS \tag{6}$$

*j*th node on the boundary of S_j. To make it more convenient, the following quantity is defined:

$$\bar{g} = \frac{\partial g}{\partial n}. \tag{7}$$

By substituting such $\bar{g}$ in (7) and *v* in (2) above into (6), the equation of Helmholtz problem now becomes

$$cp_i - \sum_{j=1}^{N} \int_{S_j} p_j \bar{g} dS = \hat{i}\rho\omega \sum_{j=1}^{N} \int_{S_j} g v_j dS. \tag{8}$$

Following by [1] with a constant element, *p* and *v* in (8) are assumed to be constant over each element. In addition, $c = 1/2$ is taken into account due to the behavior situation of (5) and then we obtain

$$\frac{1}{2} p_i - \sum_{j=1}^{N} p_j \left(\int_{S_j} \bar{g} dS \right) = \hat{i}\rho\omega \sum_{j=1}^{N} v_j \left(\int_{S_j} g dS \right). \tag{9}$$

In (9), it is noted that there are two types of integrals that must be treated over the boundary element. These relate to the node *i*th, where the fundamental solution is acting to any other node *j*th. They are sometimes specified as influence coefficients formed by $\bar{H}_{ij}$, G_{ij} as follows:

$$\bar{H}_{ij} = \int_{S_j} \bar{g} dS; \quad G_{ij} = \int_{S_j} g dS. \tag{10}$$

With respect to definition in (10), equation (9) at an arbitrary node on the boundary can be rewritten as

$$\frac{1}{2} p_i - \sum_{j=1}^{N} p_j \bar{H}_{ij} = \hat{i}\rho\omega \sum_{j=1}^{N} v_j G_{ij}. \tag{11}$$

By introducing H_{ij} in terms of the Kronecker delta δ_{ij},

$$H_{ij} = \frac{1}{2}\delta_{ij} - \bar{H}_{ij}, \tag{12}$$

equation (11) can then be expressed as

$$\sum_{j=1}^{N} H_{ij} p_j = \hat{i}\rho\omega \sum_{j=1}^{N} G_{ij} v_j. \tag{13}$$

The fact that by using appropriate shape functions in the discretized boundary, i.e., in the boundary elements and applying adequate quadrature formulae for the numerical integration in (10), a system of linear equations derived from (13) can be obtained in a matrix form

$$\mathbf{Hp} = \hat{i}\rho\omega\mathbf{Gv} \tag{14}$$

or in a shorter form with $\hat{\mathbf{G}} = \hat{i}\rho\omega\mathbf{G}$, that is,

$$\mathbf{Hp} = \hat{\mathbf{G}}\mathbf{v}. \tag{15}$$

Due to the dimension of the normal velocity vector **v** may depend on the type of the boundary shape function. For simplicity, we now assume that a structure in two-dimensional space discretized into M boundary elements and with a total of N boundary nodes is considered. On the other hand, constant elements are used in the present study. Hence, the matrices **H** and **G** have dimensions of $N \times N$ and of $N \times M$, because of homogeneity, respectively, and **p** and **v** are vector having the dimensions of N and of N, respectively. From the specified boundary conditions of the system, complementary terms of the boundary acoustic pressure field or normal velocity are given. This information is employed for the rearrangement of the equation system (15). Eventually, the calculation of the remaining unknown boundary acoustic pressure and normal velocity fields, i.e., of N dimensional vector **x**, can be obtained from the solution of a system of equations. These vectors **p** and **v** given in equation (15) consist of known and unknown boundary data. Accordingly, equation (15) containing all unknowns can be rewritten in terms of a vector **x** as

$$\mathbf{Ax} = \mathbf{f}. \tag{16}$$

It is noteworthy that the concise equation (16) is straightforward to be solved. The vector **x** is made up of all unknown boundary elements of the acoustic pressure field vector **p** and the normal velocity **v** on the boundary, whereas all given known boundary normal velocity and acoustic pressure are stored in the vector **f** on the right hand side. This may be seen that the given complementary set of the acoustic pressure field **p** and the normal velocity **v** is multiplied by the corresponding rows of the influence matrices **H** and **G** in (14).

3. Inverse Procedure for Discontinuity Detection

An inverse procedure is, in general, presented in this section for the detection of a flaw or a hole in plate structures. In this case, parameters related to the location, shape, radius and area of the hole and the length and angle of flaw are the system parameters to be identified inversely. Because the procedure is the same for both problems, hence the algorithm of inverse analysis for the plate with a hole is considered.

3.1. Interpolation

This subsection is essentially called the interpolation because once the acoustic pressure fields have been computed from the BEM forward problem, the acoustics at any points inside the domain of problems can then be interpolated due to (21) below. Consequently, the influence coefficients **H** and **G** can be first determined from the following equations:

$$G_{ij} = \int_{S_j} g dS = \int_{S_j} g(|R_i - R_j|) dS = \int_{S_j} \frac{e^{-\hat{i}k|R_i - R_j|}}{4\pi|R_i - R_j|} dS, \tag{17}$$

$$H_{ij} = \frac{1}{2}\delta_{ij} - \int_{S_j} \frac{\partial g}{\partial n} dS = \frac{1}{2}\delta_{ij} - \int_{S_j} (\nabla g)^T n dS. \tag{18}$$

In the Cartesian coordinate system, G_{ij} can be expressed in (19) below:

$$G_{ij} = \int_{S_j} \frac{e^{-\hat{i}k\sqrt{(x_i - x_j)^2 + (y_i - y_j)^2}}}{4\pi\sqrt{(x_i - x_j)^2 + (y_i - y_j)^2}} dS \tag{19}$$

and the second term of H_{ij} can be described explicitly with $n = [n_x \; n_y]^T$,

$$\nabla g = \begin{bmatrix} -\dfrac{x e^{-\hat{i}k\sqrt{x^2+y^2}}}{4\pi(x^2 + y^2)}\left(\hat{i}k + \dfrac{1}{\sqrt{x^2 + y^2}}\right) \\ -\dfrac{y e^{-\hat{i}k\sqrt{x^2+y^2}}}{4\pi(x^2 + y^2)}\left(\hat{i}k + \dfrac{1}{\sqrt{x^2 + y^2}}\right) \end{bmatrix}. \tag{20}$$

The acoustic pressure p_i at any point inside boundary S of the structure by the interpolation of the BEM can also be determined by

$$p_i = \sum_{j=1}^{N} \overline{H}_{ij} p_j + \hat{i}\rho\omega \sum_{j=1}^{N} G_{ij} v_j. \tag{21}$$

3.2. Inverse procedure of the discontinuity detection

The implementation scheme of the inverse procedure is illustrated in Figure 3.1. The inverse procedure, in general, consists of two steps of forward and inverse, which are assigned as *forward problem* and *inverse problem* in the algorithm. In this algorithm, the exact solutions of the relevant problem are assumed known prior to solve problems which are employed in evaluating the error in the inverse algorithm. Hence two individual models with and without the discontinuities must be solved in the forward branch. These computed unknown acoustic pressure fields are stored in the program using for the interpolation. With the initial mesh of both models in the forward problem, two computed acoustic fields from two models are evaluated so that the cells covering the hole can be identified. For the next iterative steps, only detected cells presenting the hole are considered.

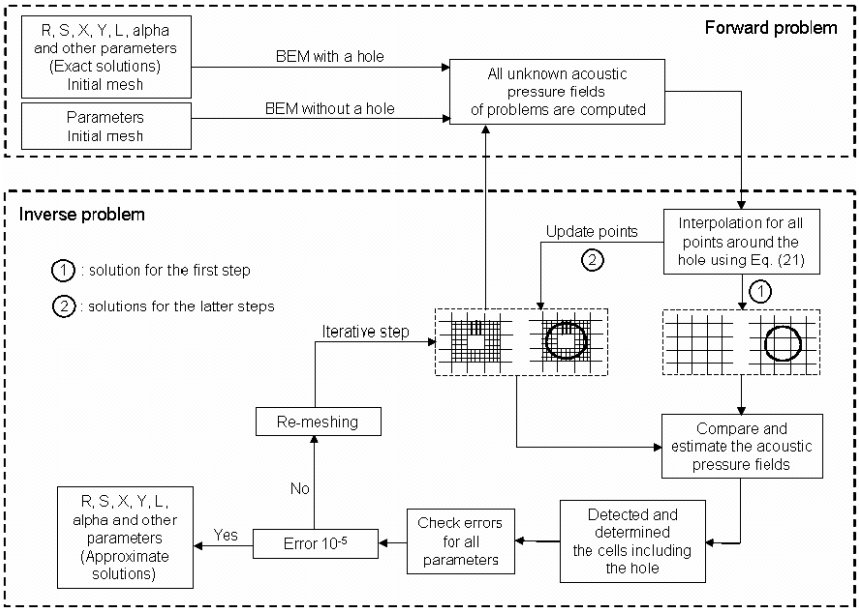

Figure 3.1. The sketch of the inverse implementation procedure for the detection of a hole within a square plate.

At each iterative step of re-meshing, the approximate solutions are compared to those of the known exact solutions. The convergence of the algorithm is based on a specified error. By determining the shape and the location of the hole, various parameters like radius, area and the centre point must be handled. In general, each parameter must be indicated by a pertinent error for the purpose of the convergence. However, for convenient, only an error of 10^{-5} is set up as a limit for the convergence of those parameters in this study. If one of them has not caught yet the specified error compared to each other, that parameter must be still in progress until its limit of convergence is reached. It is worth noting that after each iterative step of re-meshing; the detected cells involving the hole in the previous step are re-detected to find out new cells, which make the errors smaller and the solutions closer to the exact solutions. The algorithm is repeated until the solutions are reached. In fact, it may be a time-consuming task with respect to the process of making the algorithm converged.

Within the inverse method, the detected initial cells representing the hole are required by re-meshing. It is made automatically during the restart implementation procedure once considerable changes in structural shape have taken place. Within the forward problem, the selected initial cells are then subdivided by sub-cells. These sub-cells now become new cells and have the same features as the initial cells. The algorithm will then detect those new cells in order to identify new cells where the curve is currently positioned. Hence, the acoustic fields of all new cells of two models are interpolated. The identification is estimated based on the difference of total acoustic pressures at four points of a cell compared to that of each other between two models. The cells which have a minimum of total acoustic fields are picked up. This implies that the cells where the curve is located gave such a minimum of total acoustic pressures. In this estimation, the cells where the curve crossing over are detected to be used for re-meshing in the next steps. Accordingly, based on this analysis, all central points of cells are hereby determined. Furthermore, the shape of the hole is done by connecting all computed central points previously. This means that a circular hole can be computed through a set of linear piecewise connected by central points of cells by means of the interpolation of acoustic pressures in the domain. The algorithm can be seen in Figure 3.1 to get a total view how the algorithm works.

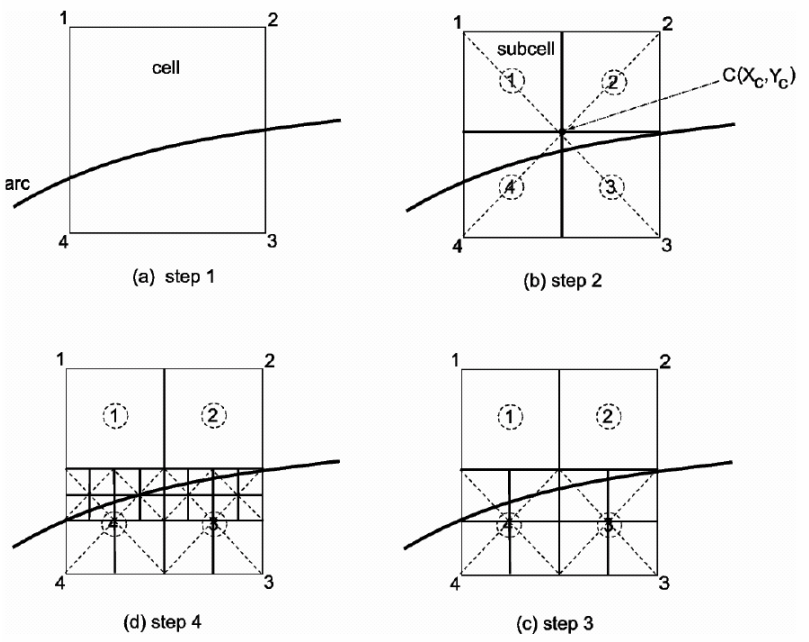

Figure 3.2. Sketch of steps for determining an arc and calculating the central points.

In other words, to clarify, Figure 3.2 above depicts several typical steps for determining the location of an arbitrary arc of a hole as well as of calculating the coordinate of central points of cell and of sub-cells. In Figure 3.2, step 1 with (a) is an initially square cell holding the arc detected by the program. This cell is determined through its four points numbered 1, 2, 3 and 4, respectively. Thus, the central point $C(X_c, Y_c)$ of the cell depicted in (b) is straightforward to compute due to equation (22) below. In (b) step 2, four sub-cells are subdivided from the initially original cell as (a). The algorithm is again detected to find new cells holding the curve. As depicted in (b), the curve now is located in two sub-cells (3) and (4). The sub-cells of (1) and (2) are no longer taken into account in next steps. Similarly, the algorithm continues to re-mesh and re-detect until the shape and location of the curve are positioned, (c) and (d) are here known as the next two steps of this algorithm. It is noted that at each iterative step of re-meshing, the acoustic fields of cells are interpolated correspondingly due to (21),

$$X_c = \sum_{i=1}^{4} \frac{X_i}{4}; \quad Y_c = \sum_{i=1}^{4} \frac{Y_i}{4}. \tag{22}$$

In addition, to calculate the length and the angle of such a nonlinear flaw, the following equations are used. For the length

$$L = \sum_{n=1}^{N_c} \sqrt{| X_{n+1} - X_n |^2 + | Y_{n+1} - Y_n |^2}, \tag{23}$$

here N_c stands for the total interpolated points within a cell and for the angle of a nonlinear flaw.

$$\alpha = \arctan\left(\frac{| Y_1 - Y_2 |}{| X_1 - X_2 |}\right) \tag{24}$$

with (X_1, Y_1) is the co-ordinate of the first point, which is analogous with the point of flaw tip and (X_2, Y_2) is the coordinate of the interpolated point closest to the first point.

4. Numerical Examples

To demonstrate and illustrate the ability of the identifying method presented above, two typical numerical problems regarding the detection of a given circular hole and a given flaw within a specified square plate are carried out, respectively. A square plate with the dimensions of 10cm × 10cm depicted in Figure 4.1 is employed. An initial acoustic source $p_0 = 5000\,\text{KHz}$ is activated at point *A* at the beginning. The speed of acoustic in medium $c = 1560\,\text{m/s}$ is given as well as the density $\rho = 1058\,\text{kg/m}^3$ is assigned [26]. The boundary conditions of the problems are treated as follows. The acoustic pressure on all boundaries of the plate is formed through the equation $p_R = p_0(1 - \sin\theta)$ with $\theta = \arcsin\left(\frac{y}{\sqrt{x^2 + y^2}}\right)$ and a normal velocity *v* described in (2) is consistently enforced, respectively.

4.1. Square plate with a circular hole

A plate with a hole shown in Figure 4.1 (right) is considered. The hole has a radius $R_c = 0.5\text{cm}$ located at the center of the square plate $C(X_C, Y_C)$. As mentioned earlier, this present inverse technique is studied as a pilot project. This implies that the prior hole is assumed to be known. To provide the data for identifying of the method, two individual models with and without the hole are carried out simultaneously. The boundaries of the square plate are discretized with 8

elements, 8 nodes and 16 double nodes depicted in Figure 4.1 (left). In the domain of the plate, an initial square mesh of 12×12 is discretized. In our inverse analysis, a cell for re-meshing is subdivided into a size of 4×4 for each iterative step.

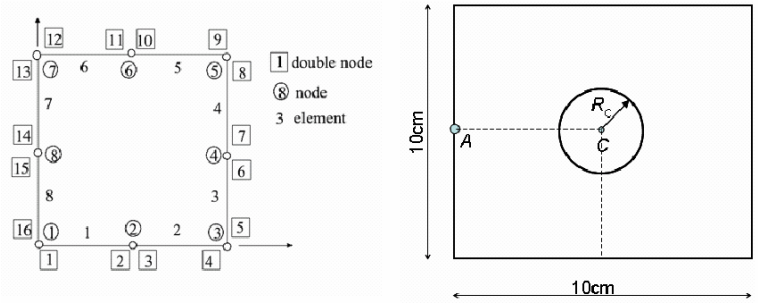

Figure 4.1. The BEM discretization of a square plate (left). A square plate with a hole (right).

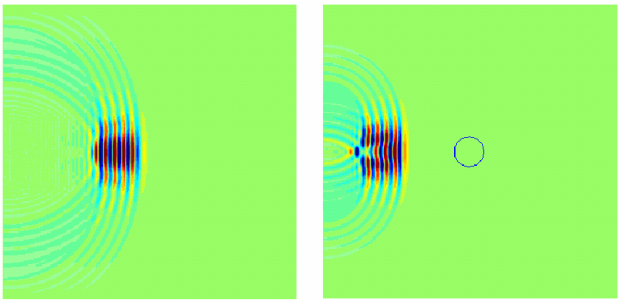

Figure 4.2. Acoustic pressure fields transfer in the plate without a hole (left) and with a hole but the hole was not touched yet (right).

Figure 4.2 (left) definitely simulates the transferring of the acoustic pressure in the smoothing plate without the hole. An acoustic pressure was transferred at the point *A* in the beginning. This test was executed in order to see how the acoustic source transfers in the domain without any discontinuities. The only important thing can be seen here that why the analysis without the hold was examined additionally. This analysis with not a hole must be carried out parallel with the one to which a hole is held. This was done because their results are required in the algorithm to estimate the loss of the acoustic pressure fields at surrounding region of the hole, so that the hole can be identified. Consequently, in contrast to Figure 4.2 (left), Figure 4.2 (right) shows a result of transferring of the acoustic pressure in the plate without detecting the hole. This can be distinct with the following cases where the acoustics are passed through the hole.

Similarly, Figure 4.3 shows two different positions of the acoustic pressure passing across the hole. The picture on the left hand side shows the acoustic source touched the hole. The acoustics at that time are pulled out and spreading into two different sides. The information regarding the location of the hole is being identified by the inverse algorithm. All information of cells covering the hole is identified and stored in the program. These cells will be re-meshed within the inverse algorithm, so that the shape as well as other relevant parameters can be determined.

The identified results of the hole such as the coordinate of the central point, area and the radius of the hole are given in Table I at three different iterative steps of re-meshing of the cells. The obtained results of the coordinate of the central point, radius and area of the hole are also presented in Figures 4.4, 4.5 and 4.6, respectively. The error is the difference between the exact and approximate solutions, which is also given in the same table.

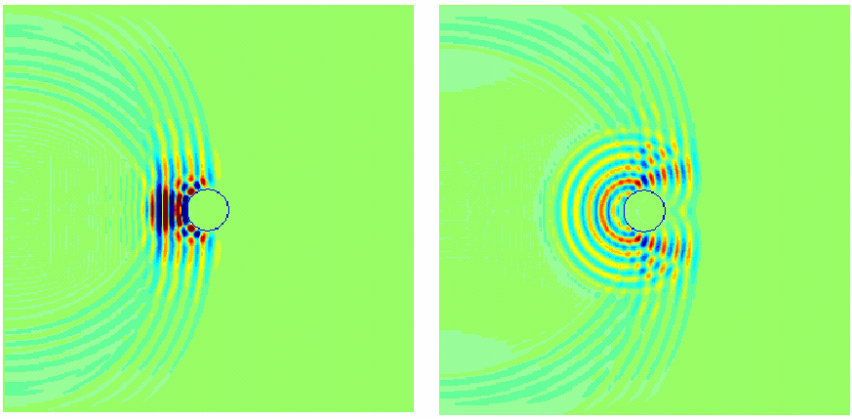

Figure 4.3. The acoustic pressure passed across the hole at two different positions.

Based on the achieved results presented above, we see that the solutions were not well converged with the first iterative step. This corresponds to the first estimation of the loss of the acoustic pressure surrounding the hole as well as the hole is just detected through a set of identified cells. As presented in Section 3 of the inverse algorithm, only detected cells are then re-meshed and the solutions of the problem are increased based on the number of iterative steps of re-meshing until the solutions are reached. Accordingly, the reasonable solutions are reached at the iterative step of $h = 10$.

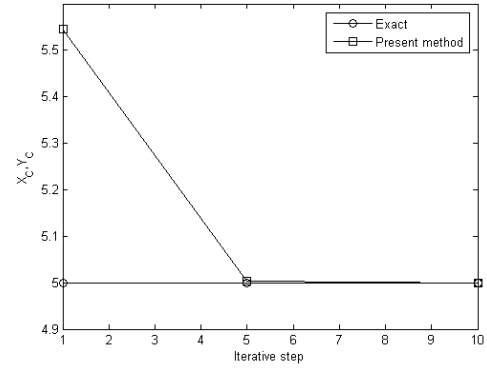

Figure 4.4. Convergence of point X_C, Y_C.

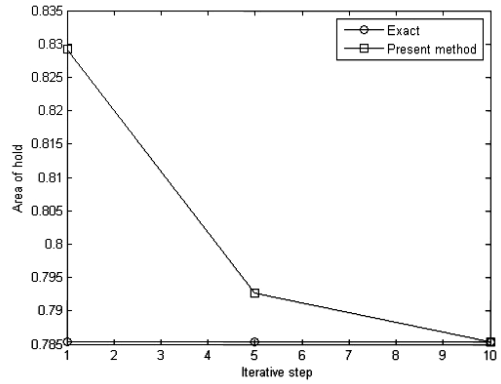

Figure 4.5. Convergence of area of the hole *S*.

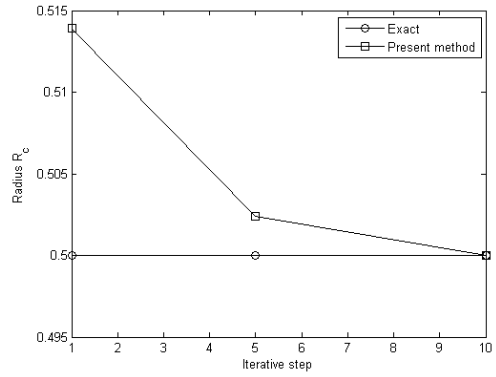

Figure 4.6. Convergence of radius R_c.

Table I. Identified results of the present method for central point, area of the hole, and radius of the square plate with a hole

Iterative step of re-meshing of the cells	Parameters	Approximate solutions of the present method	Exact solution	Error
$h = 1$	X_c	5.54597	5.00000	0.09844
	Y_c	5.54597	5.00000	0.09844
	S	0.82923	0.78547	0.05333
	R	0.51389	0.50000	0.02703
$h = 5$	X_c	5.00239	5.00000	0.00047
	Y_c	5.00239	5.00000	0.00047
	S	0.79264	0.78547	0.00963
	R	0.50242	0.50000	0.00482
$h = 10$	X_c	5.00003	5.00000	0.00001
	Y_c	5.00003	5.00000	0.00001
	S	0.78553	0.78547	0.00004
	R	0.50001	0.50000	0.00002

4.2. Square plate with a flaw

Similar to the problem of the hole investigated above, another example related a square plate consisting of a nonlinear flaw is considered. The parameters regarding the acoustic pressure, the boundary conditions and others are also taken the same as above. The procedure for the detection of this problem is analogously carried out as the hole example. The hole is now replaced by an existing flaw instead. The nonlinear flaw is also assumed to be known. The given length of flaw is specified by $L = 2.347\text{cm}$ in length through two corresponding nodes and the angle of the flaw compared to *x*-axis is also indicated by $\alpha = 45^\circ$ depicted in Figure 4.7.

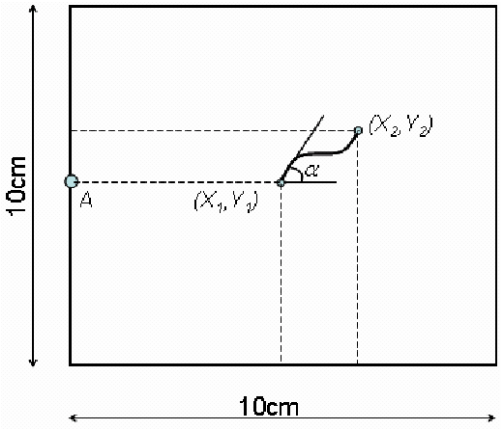

Figure 4.7. A square plate included a nonlinear flaw.

In this one, in order to interpret the shape and the location of the flaw, the coordinate values of two nodes, the length and the angle depicted in Figure 4.7, are known as unknown parameters of problem, which need to be determined. By the same situation, Figure 4.8 shows an acoustic field transfers in the plate with and without a nonlinear flaw. The identified results of the coordinate values of two nodes, the length and the angle are given in Table II. The convergences of the length and the angle of the nonlinear flaw are additionally given in Figures 4.9 and 4.10, respectively. In this analysis, it can be seen that the problem can be reached the exact solutions very well with an iterative step of $h = 10$.

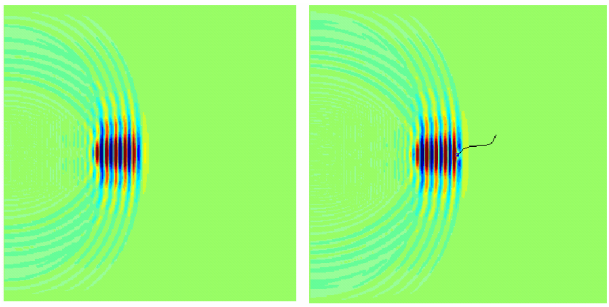

Figure 4.8. Acoustic fields passed across the plate without flaw (left) and with a nonlinear flaw (right).

Through the identified results of two numerical examples investigated above, it shows that the procedure of inverse analysis worked very well. With a prior assumption of existence of a hole or a nonlinear flaw in an elastic structure of the

plate, these hole and flaw can be identified by the proposed technique precisely. With the current situation of the method on the convergence of numerical results above, even though all the selected cells required a number of re-meshing, the problem was well converged based on a specified error. However, the re-meshing in this investigation may be a time-consuming task in the computation. For each iterative step, a new mesh of the cells is hereby required. This re-meshing technique is automatically treated inside the program. Accordingly, as a pilot problem, this inverse procedure was successfully proposed.

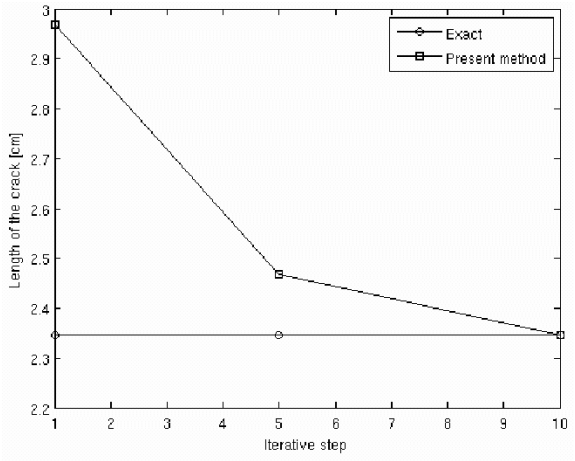

Figure 4.9. Convergence of the length of the nonlinear flaw.

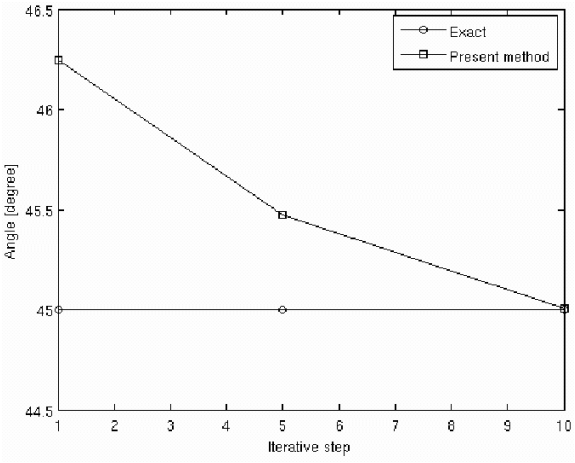

Figure 4.10. Convergence of the angle of the nonlinear flaw.

Table II. Identified results of the present method for (X_1, Y_1), (X_2, Y_2), length of the crack and the angle of the square plate with a crack

Iterative step	Parameters	Approximate solutions of the present method	Exact solution	Error
$h = 1$	X_1	4.58333	5.00000	-0.09091
	Y_1	4.58333	5.00000	-0.09091
	X_2	6.24999	5.89300	0.05712
	Y_2	7.08329	6.72400	0.05072
	L	2.96872	2.34700	0.20942
	α (degree)	46.24568	45	0.02694
$h = 5$	X_1	5.00782	5.00000	0.00156
	Y_1	5.00782	5.00000	0.00156
	X_2	5.89923	5.89300	0.00106
	Y_2	6.73071	6.72400	0.00100
	L	2.46814	2.34700	0.04908
	α (degree)	45.47211	45	0.01038
$h = 10$	X_1	5.00006	5.00000	0.00001
	Y_1	5.00006	5.00000	0.00001
	X_2	5.89308	5.89300	0.00001
	Y_2	6.72403	6.72400	0.00000
	L	2.34708	2.34700	0.00004

5. Conclusions

A procedure of inverse analysis based on the BEM for identifying the location, shape and length as well as angle of a hole or a flaw in acoustic media was proposed. Two examples detecting a nonlinear flaw and a hole within a square plate in two-dimensional space in acoustic media were illustrated. The investigated results showed in the numerical part have demonstrated the effectiveness of the proposed method. Based on the good correlation of the achieved results of the present method, obviously, an extension to other pertinent problems in the context of acoustic media following by the proposed inverse method is in principle possible. Pilot problems can, in particular, be detected once the prior existence of a nonlinear flaw or a hole is assumed to be known. In general, the method must be improved so that an arbitrary discontinuity can be identified without any initial specification.

Nevertheless, the presented study may be filled up in the area of the BEM as well as in the sphere of discontinuity detection problems. The approach would be promising to developing for further applications. Soon after, a close application to heat transfer problems using the same approach is studied by Cao and Bui [27]. A class of other problems can also be treated in such a way for 3D structures and so on. In addition, alternative interest direction could be worked out by developing other numerical methods such as meshfree methods, X-FEM, etc., in acoustic media problem.

Acknowledgments

The authors would like to acknowledge Professor Hung Nguyen-Dang, Department of Aerospace Engineering, University of Liège, Belgium, for his useful discussion.

References

[1] J. T. Katsikadelis, Boundary Elements: Theory and Applications, Elsevier Sciences, Oxford, UK, 2002.

[2] A. A. Becker, The Boundary Element Method in Engineering – A Complete Course, McGraw-Hill, UK, 1992.

[3] K. J. Bathe, Finite Element Procedures, Prentice-Hall, New Jersey, USA, 1996.

[4] T. Belytschko and T. Black, Elastic crack growth in finite elements with minimal remeshing, Internat. J. Numer. Methods Engrg. 45 (1999), 601-620.

[5] N. Moës, J. Dolbow and T. Belytschko, A finite element method for crack growth without remeshing, Internat. J. Numer. Methods Engrg. 46 (1999), 131-150.

[6] T. Belytschko, Y. Y. Lu and L. Gu, Element free Galerkin method, Internat. J. Numer. Methods Engrg. 37 (1994), 229-256.

[7] T. Q. Bui, T. N. Nguyen and H. Nguyen-Dang, A moving Kriging interpolation-based meshless method for numerical simulation of Kirchhoff plate problems, Internat. J. Numer. Methods Engrg. 77 (2009), 1371-1395.

[8] K. W. Man, Contact Mechanics using Boundary Elements, Computational Mechanics Publications, Great Britain, 1994.

[9] Q. Qing-Hua, Green's Functions and Boundary Elements of Multifield Materials, Elsevier Science, Oxford, 2007.

[10] M. Schanz and O. Steinbach, Boundary Element Analysis – Mathematical Aspects and Applications, Springer-Verlag, Berlin, Heidelberg, 2007.

[11] A. Chandra and S. Mukherjee, Boundary Element Methods in Manufacturing, Oxford University Press, New York, USA, 1997.

[12] R. D. Ciskowski and C. A. Brebbia, Boundary Element Methods in Acoustics, Springer, England, 1991.

[13] S. Marburg and B. Nolte, Computational Acoustics of Noise Propagation in Fluids-Finite and Boundary Element Methods, Springer-Verlag, Berlin, Heidelberg, 2008.

[14] S. Kirkup, The Boundary Element Methods in Acoustics, Integrated Sound Software, 2007.

[15] A. H. D. Cheng and D. T. Cheng, Heritage and early history of the boundary element method, Engineering Analysis with Boundary Elements 29 (2005), 268-302.

[16] N. Nishimura and S. Kobayashi, A boundary integral equation method for an inverse problem related to crack detection, Internat. J. Numer. Methods Engrg. 32 (1991), 1371-1387.

[17] L. M. Bezerra and S. Saigal, A boundary element formulation for the inverse elastostatics problem (IESP) of flaw detection, Internat. J. Numer. Methods Engrg. 36 (1993), 2189-2202.

[18] S. C. Mellings and M. H. Aliabadi, Flaw identification using the boundary element method, Internat. J. Numer. Methods Engrg. 38 (1995), 399-419.

[19] G. E. Stavroulakis and H. Antes, Flaw identification in elastomechanics: BEM simulation with local and genetic optimization, Structural Optimization 16 (1998), 162-175.

[20] G. E. Stavroulakis and H. Antes, Neural crack identification in steady state elastodynamics, Comput. Methods Appl. Mech. Engrg. 165 (1998), 129-146.

[21] R. Lazarovitch, D. Rittel and I. Bucher, Experimental crack identification using electrical impedance tomography, NDT & E International 35 (2002), 301-316.

[22] K. A. Woodbury, Inverse Engineering Handbook, CRC Press, USA, 2002.

[23] T. D. Cao, Studies on heat transfer and structural acoustics problems by boundary element methods, Master Thesis, University of Liège, Belgium, 2007.

[24] G. Beer and J. O. Watson, Introduction to Finite and Boundary Element Methods for Engineers, John Wiley & Sons, USA, 1994.

[25] G. Beer, I. Smith and C. Duenser, The Boundary Element Method with Programming for Engineers and Scientists, Springer, Germany, 2008.

[26] C. Pozrikidis, A Practical Guide to Boundary Element Methods with the Software Library BEMLIB, Chapman & Hall/CRC, USA, 2002.

[27] T. D. Cao and T. Q. Bui, Heat transfer problems in acoustic media based on an inverse method incorporated the boundary element method, Engineering Analysis with Boundary Elements, in preparation.